

Measurement of Two Solvation Regimes in Water-Ethanol Mixtures Using X-Ray Compton Scattering

I. Juurinen,¹ K. Nakahara,² N. Ando,² T. Nishiumi,² H. Seto,² N. Yoshida,² T. Morinaga,² M. Itou,³ T. Ninomiya,³ Y. Sakurai,³ E. Salonen,⁴ K. Nordlund,¹ K. Hämäläinen,¹ and M. Hakala^{1,*}

¹*Department of Physics, P.O. Box 64, FI-00014 University of Helsinki, Finland*

²*Process Development Department, Suntory Business Expert Limited, 57 Imaikami, Nakahara, Kawasaki 211-0067, Japan*

³*JASRI, SPring-8, 1-1-1, Kouto, Sayo-gun, Hyogo 679-5198, Japan*

⁴*Department of Applied Physics, Aalto University School of Science and Technology, P.O. Box 11100, FI-00076 Aalto, Finland*
(Received 28 October 2010; revised manuscript received 17 June 2011; published 31 October 2011)

Water-ethanol mixtures exhibit interesting anomalies in their macroscopic properties. Despite a lot of research, the origin of the anomalies and the microscopic structure itself is still far from completely known. We have utilized the synchrotron x-ray Compton scattering technique to elucidate the structure of aqueous ethanol from a new experimental perspective. The technique is uniquely sensitive to the local molecular geometries at the angstrom and subangstrom scales. The experiments reveal two distinct mixing regimes in terms of geometry: the dilute 5 mol % and the concentrated >15 mol % regimes. By comparing with pure liquids, the former regime is characterized by an intramolecular and the latter by an intermolecular change. The findings bring new light to evaluating the hypothesis of formation of clathratelike structures at the dilute concentrations.

DOI: 10.1103/PhysRevLett.107.197401

PACS numbers: 78.70.Ck, 33.15.Dj, 61.25.Em

Water-ethanol mixtures are scientifically intriguing and important for many fields ranging from basic molecular research to widespread industrial applications including beverages and biofuel. Alcohols and water mix incompletely, which is a phenomenon described in terms of negative excess entropy [1]. Related to the incomplete mixing, moreover, distinct solvation regimes as a function of ethanol concentration have been experimentally reported [2–8]. Computational studies have focused on examining the so-called “clathrate” (also known as “iceberg”) model [9] for the water-ethanol mixture and the nature of the hydrophobic hydration [10–12]. However, still no consensus exists on the precise microscopic picture at the molecular level [12]. In this Letter, we report a new molecular level experiment on aqueous ethanol to clarify its microscopic nature.

The experimental evidence of distinct solvation regimes is broad. Differential scanning calorimetry studies [2] suggested four regimes; the transition point between the first two regimes was around 15% (ethanol mole fraction hereafter), while other transition points were at 65% and 85%. These findings were in agreement with earlier NMR and Fourier-transform infrared studies [3]. Low-frequency Raman spectroscopy [4] revealed a change in the local structure at the concentration 20%. Mass spectroscopy of clusters generated from various ethanol-water mixtures (see, e.g., Refs. [5,6]) suggested three regimes, the transition points between them being at $\sim(3.3\text{--}7.1)\%$ and $\sim 73.7\%$. Absorption and emission studies showed the transition in the region of 10%–20% [7], while Raman studies [8] on stretching bands pointed to a structural rearrangement at 5.5%–10%. The prior computational

studies of aqueous ethanol have been predominantly classical molecular dynamics (MD) simulations [11–15]. van Erp and Meijer reported Car-Parrinello MD results for a single solvated ethanol molecule [10].

In this Letter, we corroborate the existence of distinct solvation regimes and provide new qualitative and quantitative information on their microscopic nature. We use the Compton scattering method [16], in which inelastically scattered x-ray photons from the sample are observed. The experiments are combined with calculations based on model molecular clusters to interpret and rationalize the findings. In Compton scattering the photon scattering cross section is extremely sensitive to any changes in the intra- and intermolecular bond lengths in the subangstrom scale [17,18]. For molecular systems, Compton scattering probes, for example, changes in the hydrogen bond topologies between different thermodynamic conditions [19–24] or concentrations [25].

In the x-ray Compton scattering setup, the incident photon energy is far from the resonances of the system, and there is a large energy and momentum transfer from the photon to the electrons of the target [26,27]. Within the impulse approximation [28], the experimentally measured scattering cross section from an isotropic system is proportional to the Compton profile $J(q)$, which is determined by the ground-state electronic structure of the system. The experiment was performed at the BL08W beam line [29] of SPring-8. The liquid samples were confined in an Al holder with 10 μm thick Kapton films as x-ray windows and placed in a vacuum chamber. The ethanol concentrations were 5.5, 15.7, 30.9, 53.2, and 73.1 mol % (20, 40, 60, 80, and 90 vol %, respectively). The sample shape was 10 mm

in diameter and 10 mm in thickness along the incident x rays. The incident x-ray energy was 176.3 keV, and the scattering angle was 178.3° . Compton-scattered x rays around 104 keV were detected by a 10-element Ge solid-state detector with an overall momentum resolution of 0.56 atomic units (a.u.). Since large statistics is needed to resolve subtle features in the Compton profiles, the nature of the experiment is very demanding. The backgrounds were measured by placing the empty holder in the chamber and subtracted from the measured spectra. All the measurements were carried out at room temperature. The measured spectra were corrected for the necessary energy-dependent corrections such as absorption, detection efficiency, and scattering cross section. The contribution of multiple scattering in the sample was evaluated by a Monte Carlo simulation and subtracted from the corrected profiles.

The Compton profile for liquid samples corresponds to the integral [26]

$$J(q) = \frac{1}{2} \int_{|q|}^{\infty} \int_0^{2\pi} \int_0^{\pi} \langle n(\mathbf{p}) \rangle \sin\theta \, d\theta \, d\phi \, p \, dp, \quad (1)$$

where $\langle n(\mathbf{p}) \rangle$ is the time-averaged electronic momentum density of the liquid and q a scalar momentum variable. $J(q)$ is normalized according to the number of electrons. The momentum density and the Compton profile are obtained as sums of the Fourier-transformed single-particle electron wave functions [30]. The computations have been done within the density-functional theory using the StoBe-deMon software with a cluster approach [30,31].

The observable that we will use in the analysis is the difference Compton profile

$$\Delta J(q) = J_x(q) - [xJ_{\text{EtOH}}(q) + (1-x)J_{\text{H}_2\text{O}}(q)], \quad (2)$$

where $J_x(q)$ is the Compton profile of the mixture and $xJ_{\text{EtOH}}(q) + (1-x)J_{\text{H}_2\text{O}}(q)$ is the weighted sum of the Compton profiles of pure water and ethanol. x is the molar fraction of ethanol in the mixture. The observable reveals the change in the valence electron structure of the mixture relative to that of the pure reference liquids.

Classical molecular dynamics simulations were performed to generate starting molecular coordinates for the analysis and interpretation of the experimental data. The Gromacs software [32] and standard four-point transferable intermolecular potential [33] and all-atom optimized potentials for liquid simulations [34] force fields were used to generate the pure liquids and their mixtures. The commonly studied quantities (densities, radial distribution functions, and numbers of H bonds) were similar to experiments and other corresponding simulations [10,11,13–15]. Clusters of 10–20 molecules were extracted from the MD structures for the subsequent calculation of Compton profiles. The 5%, 15%, and 95% mixtures were considered. The comparison of the obtained Compton profiles to the experimental data according to Eq. (2) showed, however, a rather strong disagreement. The calculated $\Delta J(q)$ curves

were roughly 3 times smaller in amplitude and incorrect in shape. This disagreement was partially expected, since the O-H bond length of water was fixed and polarizability was not included in the force field.

In order to explain the experimental data, we have carried out a systematic further analysis by modifying these starting configurations. The most important features in $\Delta J(q)$ arise from two factors: changes in intramolecular covalent bond lengths (C-C, C-O, C-H, or O-H) and changes in intermolecular nearest-neighbor distances [19,25,35,36]. The former affect the Compton profile strongly because the wave functions forming the covalent bonds are very sensitive to the positions of the nuclei. The latter influence is due to the exchange repulsion and charge transfer between the neighboring molecules [30,35]. Changes in the H-O-H or O...H-O angles induce much weaker features in $\Delta J(q)$ and were not considered further in this work [36]. Moreover, in ethanol the O-H part is the functional group, while the covalent bonds C-C, C-O, and C-H are not expected to change appreciably between the pure liquid and the mixture phases. In Raman, IR, and NMR experiments, the most interesting behavior is typically found for O-H [3,37]. We thus choose as the framework of interpretation of the experimental data the following: analysis of changes in the intramolecular O-H bond lengths of both water and ethanol and analysis of changes in the intermolecular distances between the molecules. The first was calculated with clusters with all the O-H bonds modified and the second with clusters where all the molecules were moved with respect to a molecule in the center of the cluster. Figure 1 illustrates schematically this approach.

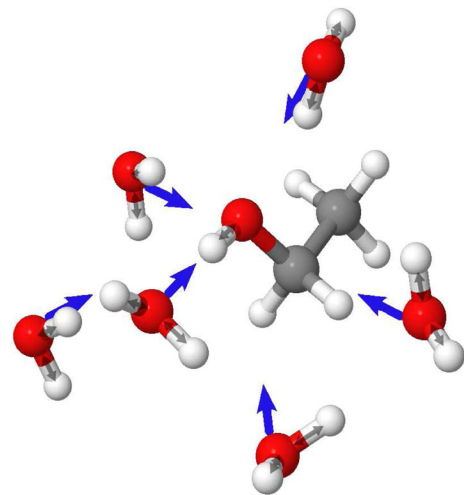


FIG. 1 (color online). Example of a configuration (all the molecules not shown) extracted from the molecular dynamics simulation. Large arrows (blue) point to the center of the cluster and indicate the direction along which the molecules were moved for simulating a density increase in the mixture. Small arrows (gray) indicate O-H bond lengths that were modified to simulate intramolecular changes.

The main results from the analysis of the modified clusters are presented in Fig. 2. Case (a) shows that if any of the intramolecular covalent bond lengths is elongated (O-H of water or ethanol and C-O, C-C, and C-H of ethanol), this leads to a broad feature in $\Delta J(q)$. If the elongation is of the same amount, the features are similar and cannot be distinguished from each other within the limit set by the experimental error bar (i.e., within roughly 0.02% units). For the O-H bond length we also tested that the $\Delta J(q)$ feature is practically the same independent of whether a single O-H bond was elongated by a Å or n O-H bonds were elongated by a/n Å in a cluster. Case (b) in Fig. 2 demonstrates that a qualitatively different, faster oscillation follows by contracting the nearest-neighbor distances but keeping the intramolecular geometries unaltered. In other words, case (b) shows the effect of density increase relative to pure liquids. The features observed in this analysis are similar to previously reported findings for water systems [36].

The experimental data are presented in Fig. 3 with selected model calculations. The 5.5% (20 vol %) data (denoted in the following as the dilute regime) are strikingly different from the 15.7%–73.1% (40–90 vol %) ones (ethanol-rich regime). The transition observed in Compton scattering is thus in the range $\sim(6\text{--}15)\%$. The observation of this transition supports the previous findings of different solvation regimes at lower concentrations [2–8]. The four cases in the ethanol-rich regime cannot be distinguished from each other within experimental uncertainties. By comparing the experimental data to Fig. 2, visual

inspection readily informs about the geometrical main characteristics of the regimes: The dilute regime is characterized by intramolecular elongations and the ethanol-rich by intermolecular contractions relative to pure liquids.

The experimental data can be also compared to previous results from aqueous systems. The 5.5% curve is broad and has a shape similar to that which occurs when the O-H bond length in pure water changes [20]. In contrast, the experimental curves 15.7%–73.1%, in addition to starting from the opposite side of the zero line, have a significant difference in their shape as compared to the dilute case: Above $q = 1.5$ a.u. the curves are practically zero. This behavior is typical in the cases that the predominant effect is an average change in the intermolecular distances [19,23]. However, it is important to stress that these are the major qualitative characteristics. Because of the large experimental uncertainties, other minor geometrical changes can take place (e.g., some density change in the dilute regime relative to pure liquids).

In the dilute regime, we find that the mean O-H elongation has to be of the order of 0.003 Å relative to pure liquids. The model curve shown in Fig. 3 is obtained by elongating all the O-H bonds of the clusters in the 5% mixture by this amount. As discussed above, the result is independent of which intramolecular bonds are elongated, provided that the mean elongation stays the same. However, one can rule out at least two cases. First, the O-H of the ethanol cannot be the only bond to change, since this would require a physically too large elongation

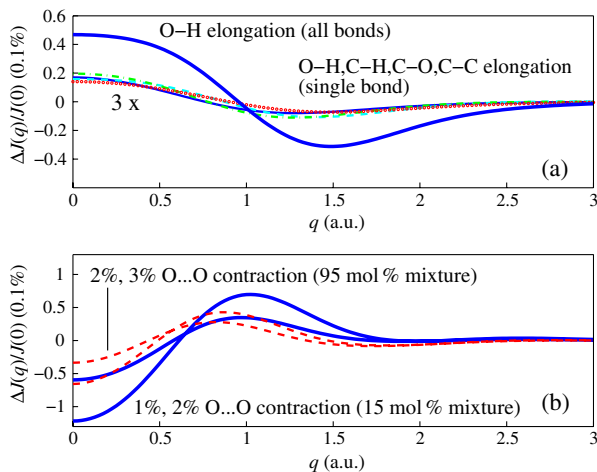


FIG. 2 (color online). (a) Changes in the Compton profile when all the intramolecular O-H bond lengths are increased by 0.003 Å (blue solid line) and one bond [O-H of water or ethanol (red), C-O (cyan), C-C (green), or C-H (blue)] in a cluster increased by 0.01 Å (latter multiplied by 3 for better clarity). (b) Changes in the Compton profile when the density increases: intermolecular O...O distances decreased by 1% and 2% (for 15% mixture) and 2% and 3% (for 95% mixture). For both concentrations, larger features arise for larger contractions.

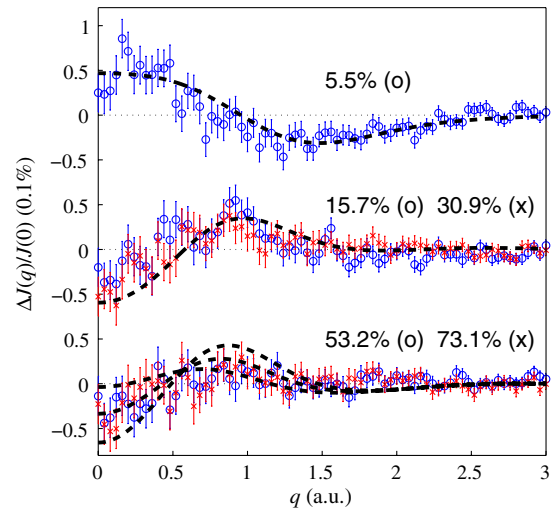


FIG. 3 (color online). Experimental Compton profile differences from Eq. (2). The experimental data are given by red crosses (\times) and blue circles (\circ). The molar percentages of ethanol have been indicated, and the data have been shifted for clarity. The black dashed curves are model calculations from modified MD clusters. Uppermost curve: O-H bonds elongated by 0.003 Å in the 5% mixtures; middle curve: O...O distances decreased by 1% in the 15% mixtures; lowermost three curves: O...O distances decreased by 1%, 2%, and 3% in the 95% mixtures.

(of the order of 0.1 Å). Second, on the same grounds one can rule out that the elongation concerned only those O-H groups of water which are directly H-bonded to ethanol. Since water has roughly 2.2 H bonds with ethanol [11], this would require the directly H-bonded water molecules to have ~ 0.06 Å longer O-H bonds compared to the average value in pure water. This elongation appears again physically too large. Therefore, the only plausible explanation is that all the O-H bonds are affected to some extent throughout the liquid.

The experimental observation at the dilute regime can be also compared to those by Burikov *et al.* [8,37] They reported the maximal strength of H-bonding at the dilute regime 6.5%–9% (14–20 vol %) by Raman and IR spectroscopy. The strengthening of H-bonding is correlative to shorter O-H...O bonds and longer intramolecular O-H bonds [38]. In the case of the Compton profile of water, the O-H bond length was found inversely proportional to the O-H...O distance [25]. Our observation of the mean O-H elongation in the dilute regime is thus in agreement with the strong H bonds found by Burikov *et al.* Noskov, Lamoureux, and Roux [11] provide an interesting additional aspect: They reported by classical molecular dynamics that particularly at the dilute 5% concentration an excess of H-bonding can persist even until 8 Å distance from the ethanol molecules.

At the ethanol-rich regime, the present experiment indicates that the intermolecular contraction relative to pure liquids becomes the predominant effect. The model curves shown in Fig. 3 suggest that the density increase relative to pure liquids is of the order of 1%–3%. (Since we consider clusters instead of periodic systems, the true density increase is less than that calculated from the used O...O contraction.) Our finding is in good agreement with the experimental values for the density increase: 1.2%–2.2% at 15.7%–73.1% (0.7% at 5.5%) [39].

The microscopic structure of aqueous ethanol revealed by Compton scattering is intriguing, and we confirm the structural rearrangement taking place between concentrations 6% and 15%. To explain the present results, we found no need to evoke the concept of clathratelike structures in the dilute regime. It is worthwhile to emphasize that the observed differences in the mean distances are extremely small between the dilute and concentrated regimes.

In conclusion, we report by the experimental synchrotron-based x-ray Compton scattering method the properties of two microscopic mixing regimes in water-ethanol solutions. Relative to pure liquids, the dilute regime is characterized predominantly by an increase of the intramolecular bond lengths, while the ethanol-rich regime is characterized by the excess density. However, the observed average structural rearrangement between the dilute and ethanol-rich regimes is very small in terms of characteristic atomic distances. Therefore, the experimental data contain no hints of any anomalous structural motifs

such as the clathratelike formation. With this work the Compton scattering method shows its unique strength as a means to assess subtle geometrical features in liquid structures. The foreseen future applications are, e.g., probing of water in nanostructures and characterization of the hydration and self-interaction properties of polymers and proteins.

The experiment at SPring-8 was approved by JASRI, Proposals No. 2006A0201 and No. 2007A1378. This work has been supported by the Academy of Finland [NGSMP, Contract No. 1127462 and the Centers of Excellence Program (2006–2011)] and the Research Funds of the University of Helsinki. We thank J. Lehtola and A. Sakko for discussions.

*Mikko.O.Hakala@helsinki.fi

- [1] S. Dixit, J. Crain, W. C. K. Poon, J. L. Finney, and A. K. Soper, *Nature (London)* **416**, 829 (2002).
- [2] K. Takaizumi and T. Wakabayashi, *J. Solution Chem.* **26**, 927 (1997).
- [3] K. Mizuno, Y. Miyashita, Y. Shindo, and H. Ogawa, *J. Phys. Chem.* **99**, 3225 (1995).
- [4] K. Egashira and N. Nishi, *J. Phys. Chem. B* **102**, 4054 (1998).
- [5] N. Nishi, K. Koga, C. Ohsima, K. Yamamoto, U. Nagashima, and K. Nagami, *J. Am. Chem. Soc.* **110**, 5246 (1988).
- [6] A. Wakisaka and K. Matsuura, *J. Mol. Liq.* **129**, 25 (2006).
- [7] T. Pradhan, P. Ghoshal, and R. Biswas, *J. Chem. Sci.* **120**, 275 (2008).
- [8] S. Burikov, S. Dolenko, T. Dolenko, S. Patsaeva, and V. Yuzhakov, *Mol. Phys.* **108**, 739 (2010).
- [9] H. S. Frank and M. W. Evans, *J. Chem. Phys.* **13**, 507 (1945).
- [10] T. S. van Erp and E. J. Meijer, *J. Chem. Phys.* **118**, 8831 (2003).
- [11] S. Y. Noskov, G. Lamoureux, and B. Roux, *J. Phys. Chem. B* **109**, 6705 (2005).
- [12] Y. Zhong and S. Patel, *J. Phys. Chem. B* **113**, 767 (2009).
- [13] E. J. W. Wensink, A. C. Hoffmann, P. J. van Maaren, and D. van der Spoel, *J. Chem. Phys.* **119**, 7308 (2003).
- [14] Y. Zhang and S. Patel, *J. Phys. Chem. B* **113**, 767 (2009).
- [15] J. Fidler and P. M. Roger, *J. Phys. Chem. B* **103**, 7695 (1999).
- [16] M. J. Cooper, P. E. Mijnarends, N. Shiotani, N. Sakai, and A. Bansil, *X-ray Compton Scattering* (Oxford University, New York, 2004).
- [17] M. Hakala, K. Nygård, S. Manninen, L. G. M. Pettersson, and K. Hämäläinen, *Phys. Rev. B* **73**, 035432 (2006).
- [18] M. Hakala, K. Nygård, J. Vaara, M. Itou, Y. Sakurai, and K. Hämäläinen, *J. Chem. Phys.* **130**, 034506 (2009).
- [19] M. Hakala, K. Nygård, S. Manninen, S. Huotari, T. Buslaps, A. Nilsson, L. G. M. Pettersson, and K. Hämäläinen, *J. Chem. Phys.* **125**, 084504 (2006).

- [20] K. Nygård, M. Hakala, T. Pylkkänen, S. Manninen, T. Buslaps, M. Itou, A. Andrejczuk, Y. Sakurai, M. Odelius, and K. Hämäläinen, *J. Chem. Phys.* **126**, 154508 (2007).
- [21] K. Nygård, M. Hakala, S. Manninen, M. Itou, Y. Sakurai, and K. Hämäläinen, *Phys. Rev. Lett.* **99**, 197401 (2007).
- [22] P.H.-L. Sit, C. Bellin, B. Barbiellini, D. Testemale, J.-L. Hazemann, T. Buslaps, N. Marzari, and A. Shukla, *Phys. Rev. B* **76**, 245413 (2007).
- [23] C. Bellin, B. Barbiellini, S. Klotz, T. Buslaps, G. Rousse, T. Strässle, and A. Shukla, *Phys. Rev. B* **83**, 094117 (2011).
- [24] F. Lehmkuhler *et al.*, *J. Phys. Chem. Lett.* **1**, 2832 (2010).
- [25] K. Nygård, M. Hakala, S. Manninen, A. Andrejczuk, M. Itou, Y. Sakurai, L. G. M. Pettersson, and K. Hämäläinen, *Phys. Rev. E* **74**, 031503 (2006).
- [26] M. J. Cooper, *Rep. Prog. Phys.* **48**, 415 (1985).
- [27] *X-Ray Compton Scattering*, edited by M. J. Cooper, P. E. Mijnarends, N. Shiotani, N. Sakai, and A. Bansil (Oxford University, Oxford, 2004).
- [28] P. Eisenberger and P. M. Platzman, *Phys. Rev. A* **2**, 415 (1970).
- [29] Y. Sakurai, *J. Synchrotron Radiat.* **5**, 208 (1998).
- [30] M. Hakala, S. Huotari, K. Hämäläinen, S. Manninen, P. Wernet, A. Nilsson, and L. G. M. Pettersson, *Phys. Rev. B* **70**, 125413 (2004).
- [31] K. Hermann and L. G. M. Pettersson, StoBe-deMon version 3.0, <http://www.fhi-berlin.mpg.de/KHsoftware/StoBe/index.html>, 2009.
- [32] H. J. C. Berendsen, D. van der Spoel, and R. van Drunen, *Comput. Phys. Commun.* **91**, 43 (1995).
- [33] W. L. Jorgensen, J. Chandrasekhar, J. D. Madura, R. W. Impey, and M. L. Klein, *J. Chem. Phys.* **79**, 926 (1983).
- [34] W. L. Jorgensen, D. S. Maxwell, and J. Tirado-Rives, *J. Am. Chem. Soc.* **118**, 11 225 (1996).
- [35] T. K. Ghanty, V. N. Staroverov, P. R. Koren, and E. R. Davidson, *J. Am. Chem. Soc.* **122**, 1210 (2000).
- [36] M. Hakala, K. Nygård, S. Manninen, L. G. M. Pettersson, and K. Hämäläinen, *Phys. Rev. B* **73**, 035432 (2006).
- [37] S. Burikov, T. Dolenko, S. Patsaeva, Y. Starokurov, and V. Yuzhakov, *Mol. Phys.* **108**, 2427 (2010).
- [38] T. Steiner, *Angew. Chem., Int. Ed.* **41**, 48 (2002).
- [39] E. D. R. Lide, *CRC, Handbook of Chemistry and Physics* (CRC, Boca Raton, FL, 2001), 82nd ed.